XVI SIMPOSIO
IBEROAMERICANO
SOBRE PROTECCIÓN
DE SISTEMAS ELÉCTRICOS
DE POTENCIA

Comparative Study of Dynamic Mode Decomposition Approaches for Electromechanical Oscillation Analysis in Low Inertia Power Systems

Ramón Daniel Rodríguez-Soto[a], Emilio Barocio[b]

[a]*División de Tecnologías para la Integración Ciber-Humana. Universidad de Guadalajara. Guadalajara, Mexico*
[b]*Programa de posgrado en Ingeniería Eléctrica. Universidad de Guadalajara. Guadalajara, Mexico*

ABSTRACT

The integration of renewable energy sources into power grids introduces critical challenges related to stability and oscillatory behavior. In addition, electromagnetic oscillations, particularly low-frequency oscillations (LFOs), significantly impact grid reliability. Dynamic Mode Decomposition (DMD) methods provide valuable insights into these phenomena, identifying frequency and damping modes from electrical system measurements. In this study, we rigorously compare various DMD variants—namely, svdDMD, augDMD, fbDMD, tDMD, and rDMD—regarding their accuracy, noise robustness, and computational efficiency. Our evaluation employs a modified IEEE 39-bus test system incorporating pumped storage hydropower plants and wind power. The findings assist power system operators in selecting optimal methods for electromechanical oscillation analysis, ultimately enhancing grid stability and resilience.

Keywords: DMD, oscillation analysis, stability, styling

1. Introduction

In the swiftly changing landscape of energy systems, the incorporation of renewable energy sources presents significant challenges to the stability and dependability of power grids. As the global community experiences an increase in non-programmable renewable energy sources, operators of electric systems are obliged to reevaluate the security and robustness of power systems. This paradigm shift highlights the crucial role of sophisticated monitoring systems, especially in the context of oscillatory behaviors that can threaten the stability of interconnected networks.

A common electromechanical phenomenon affecting power systems is inter-area oscillation, which appears as oscillatory transients between remote generation systems. These oscillations, with frequencies typically ranging from 0.1 to 0.7 Hz, can lead to frequency oscillations on the transmission grid. The repercussions of inadequate damping in these oscillations can be drastic, potentially initiating cascading events and resulting in extensive blackouts [1].

To tackle these challenges, implementing Phasor Measurement Units (PMUs) in Wide-Area Monitoring Systems (WAMSs) offers real-time measurements of voltage and current phasors, frequency, and other signals. The WAMS, when combined with innovative data-driven methods, provides an effective approach to analyze low-frequency oscillations and promptly detect critical operating conditions.

Among the various data-driven methods, Dynamic Mode Decomposition (DMD) stands out as a potent tool for oscillation analysis. Originating from fluid dynamics, DMD has proven its efficiency in identifying dynamical modes and their spatial and temporal characteristics. This technique has gained rapid popularity, and a recent method, Augmented DMD (augDMD) [2] has been proposed by integrating the ideas of the standard DMD with Takens' theorem to achieve significant improvements in prediction when the time complexity exceeds the spatial complexity of a dynamic system. However, challenges and limitations are also presented. The sensitivity of DMD to noise has led to several modifications to enhance robustness against noise, such as forward-backward DMD (fbDMD), and total DMD (tDMD) [3]. Furthermore, Randomized DMD (rDMD) [4] aims at reducing computational complexity during the pre/post-processing stages of handling big data.

DMD was introduced to power systems, demonstrating its effectiveness for the modal analysis of electromagnetic oscillations, and identifying dynamical modes and their spatial and temporal characteristics [5–7].

As we traverse the complexities of the energy transition, the integration of renewable energy sources requires not only enhanced monitoring capabilities but also advanced methodologies, such as

DMD, to ensure the stability and resilience of power grids in the face of dynamic challenges. This work delves into a comparative study of the applications of DMD and the significance of monitoring oscillations, particularly inter-area oscillations, and improving monitoring efficiency.

2. Techniques of Dynamic Mode Decomposition

Dynamic Mode Decomposition (DMD) is a data-driven methodology that finds its roots in the theory of the Koopman operator[8]. Initially developed for fluid dynamics by Schmid[9], DMD has demonstrated its adaptability in breaking down complex flows into coherent space-time structures. The technique excels in pinpointing Koopman modes from spatio-temporal data, where each mode embodies a distinct frequency and growth rate, signifying a non-linear extension of the global eigenmodes discovered in linear systems[10].

The essence of DMD is the local approximation of a dynamic system with a linear system. This is characterized by a system's state vector $\mathbf{x} \in \mathbb{R}^m$ linear discrete time-invariant dynamic system with sampling time Δt, correlates with the subsequent state $\mathbf{x}_{k+1} \in \mathbb{R}^m$ through:

$$\mathbf{x}_{k+1} = \mathbf{F}(\mathbf{x}_k) \tag{1}$$

where $\mathbf{F} \in \mathbb{R}^{m\times m}$ is the optimal DMD linear operator matrix, for $k = 1, \ldots, n-1$. The subsequent right eigenvector and continuous eigenvalues of $\mathbf{F}$ are represented as $\boldsymbol{\phi}_k$ and $\lambda_k = \exp(\omega_k \Delta t)$ respectively, provide insights into the system's dynamics[11], as seen in

$$\mathbf{x}(t) = \boldsymbol{\Phi} \exp(\boldsymbol{\Omega} t)\mathbf{a} \tag{2}$$

where the components of $\boldsymbol{\Phi} \in \mathbb{C}^{m\times m}$ are the dynamic modes of the system and $\boldsymbol{\Omega} \in \mathbb{C}^{m\times m}$ are the continuous eigenvalues matrix of $\mathbf{F}$. In contrast, the coefficients $\mathbf{a} \in \mathbb{C}^{m\times 1}$ represent the coordinates of the initial value $\mathbf{x}(0)$ in the base of the eigenvectors.

The practical application of DMD in a dynamic system involves organizing spatially distributed measurements collected at distinct n time instants, each Δt, into what are often referred to as snapshot matrices $\mathbf{X}_1 \in \mathbb{R}^{m\times n-1}$ and $\mathbf{X}_2 \in \mathbb{R}^{m\times n-1}$ given by

$$\mathbf{X}_1 = \begin{bmatrix} x_{1,1} & x_{1,2} & \cdots & x_{1,n-1} \\ x_{2,1} & x_{2,2} & \cdots & x_{2,n-1} \\ \vdots & \vdots & \vdots & \\ x_{m,1} & x_{m,1} & \cdots & x_{m,n-1} \end{bmatrix} \tag{3}$$

$$\mathbf{X}_2 = \begin{bmatrix} x_{1,2} & x_{1,3} & \cdots & x_{1,n} \\ x_{2,2} & x_{2,3} & \cdots & x_{2,n} \\ \vdots & \vdots & \vdots & \\ x_{m,2} & x_{m,3} & \cdots & x_{m,n} \end{bmatrix} \tag{4}$$

Thus, the approximation of (1) can be rewritten as:

$$\mathbf{X}_2 = \mathbf{F}\mathbf{X}_1 \tag{5}$$

Hence, the matrix $\mathbf{F}$ is determined through the relation

$$\mathbf{F} = \mathbf{X}_2\mathbf{X}_1^{\dagger} \tag{6}$$

leveraging the Moore-Penrose pseudoinverse $\mathbf{X}_1^{\dagger}$. The acquired knowledge of $\mathbf{F}$ facilitates modal analysis, revealing the dynamic modes and associated parameters without relying on the explicit dynamical equations of the system.

DMD's significance lies in its sole reliance on data, eliminating the need for a priori knowledge of the system's dynamics. Several DMD variants, such as Augmented DMD (augDMD)[2], forward-backward DMD (fbDMD)[3], total DMD (tDMD)[3] and Randomized DMD (rDMD)[4], among others, have emerged in recent years. These variants have found applications in diverse fields, including power systems and the monitoring of electromagnetic oscillations[5–7]. The subsequent sections delve into the mathematical foundations of these DMD variants for computing the eigenvalues and eigenvectors of the linear operator, offering a comprehensive understanding of their practical implementation.

2.1. Orthogonal Projection in DMD Operator

The standard DMD algorithm, also known as Exact DMD, computes a finite-dimensional operator that maps each column of $\mathbf{X}_1$ to its corresponding column in $\mathbf{X}_2$ as per (5). This technique, grounded in Singular Value Decomposition (SVD), forms the foundation for computing the $\mathbf{F}$ DMD operator. The SVD decomposition applied to $\mathbf{X}_1$ results in

$$\mathbf{X}_1 = \mathbf{U}\boldsymbol{\Sigma}\mathbf{V}^T \tag{7}$$

where $\mathbf{U} \in \mathbb{R}^{m\times m}$ and $\mathbf{V}^T \in \mathbb{R}^{m\times n}$ represent the left and right singular vectors respectively, along with the diagonal singular matrix $\boldsymbol{\Sigma} \in \mathbb{R}^{m\times m}$.

Substituting (7) into (6) yields the following equation

$$\hat{\mathbf{X}}_2 = \mathbf{F}\mathbf{U}_r\boldsymbol{\Sigma}_r\mathbf{V}_r^T \tag{8}$$

$\mathbf{F}$ is the approximation matrix that shares identical eigenvalues and eigenvectors with the complete behavior of the dynamic system. As per the literature, the following expression provides a representation of $\mathbf{F}$ in the base covered by the left singular vector modes of the sequence $\mathbf{X}$:

$$\hat{\mathbf{F}} = \mathbf{U}^T\mathbf{F}\mathbf{U}^T = \mathbf{U}^T\mathbf{X}_2\mathbf{V}\boldsymbol{\Sigma}^{-1} \tag{9}$$

Computing the eigendecomposition of $\hat{\mathbf{F}}$

$$\hat{\mathbf{F}}\mathbf{W} = \mathbf{W}\boldsymbol{\Lambda} \tag{10}$$

where the columns of matrix $\mathbf{W} \in \mathbb{C}^{m\times m}$ are the eigenvectors, and $\boldsymbol{\Lambda} \in \mathbb{C}^{m\times m}$ is a diagonal matrix containing the eigenvalues λ_j of $\hat{\mathbf{F}}$. Therefore, the DMD modes are given by

$$\boldsymbol{\Psi} = \mathbf{X}\mathbf{W} \tag{11}$$

$$\boldsymbol{\Phi} = \mathbf{X}_2\mathbf{V}\boldsymbol{\Sigma}^{-1}\mathbf{W} \tag{12}$$

where $\boldsymbol{\Psi}$ are projected DMD modes and $\boldsymbol{\Phi}_i$ are referred to as exact DMD modes, $\boldsymbol{\Psi}$ and $\boldsymbol{\Phi}_i$ are equivalent when $\mathbf{X}_1$ and $\mathbf{X}_2$ span the same Δt. If $\phi_j \neq 0$, (5) may be utilized to determine the dynamic mode of $\hat{\mathbf{F}}$ associated with the k-th zero eigenvalue $\lambda_k = 0$. Alternatively, (6) should be used.

2.1.1. SVD Decomposition Derived DMD

Eigendecomposition of the low-dimensional system matrix, $\mathbf{F}$, provides an insightful explanation of system dynamic behavior; assuming the operator $\mathbf{F}$ is diagonalizable can be obtained from the modal decomposition by substituting (9), the following expression

$$\mathbf{F} = \mathbf{W}\boldsymbol{\Lambda}\mathbf{W}^{-1} = \mathbf{U}^T\mathbf{X}_2\mathbf{V}\boldsymbol{\Sigma}^{-1} \tag{13}$$

Using (1), that can be approximated by a linear combination of the DMD modes, multiplying on the left by $\mathbf{U}$ and on the right by $\boldsymbol{\Sigma}\mathbf{V}^T$, the resulting reconstructed matrix $\mathbf{X}_{2\ rec}$ as

$$\mathbf{X}_{\text{rec}}^{\text{svd}} = \mathbf{U}\mathbf{W}\boldsymbol{\Lambda}\mathbf{W}^{-1}\boldsymbol{\Sigma}\mathbf{V}^T = \boldsymbol{\Phi}\boldsymbol{\Lambda}\boldsymbol{\Gamma} \tag{14}$$

where $\mathbf{\Phi} \in \mathbb{C}^{m\times m}$ reflects the spatial term of the system's dynamic and the structure $\mathbf{\Gamma} \in \mathbb{C}^{m\times m}$ denotes the temporal evolution of the modes of the system, the technique described above is known as svdDMD.

For the identification of damping ρ_j and frequency f_j associate to mode ϕ_j can be depicted from eigenvalues λ_j the following transformation procedure is employed:

$$\rho_j = \frac{\Re(\lambda_j)}{\Delta t}, \quad f_j = \frac{\Im(\lambda_j)}{\frac{\Delta t}{2\pi}} \tag{15}$$

Alternatively, due to the spatial structure of the dynamic of the system associated with the modes of the system described as ϕ_j, the normalized magnitude of each mode $\|\phi_j\|$ can be used to determine the participation factor associated with each mode at instant t. The existing groups can be visualized with similar dynamic behavior using the phase $\angle\phi_j$.

2.2. Estimation of DMD Operator via Augmented Matrix

The Augmented Dynamic Mode Decomposition (augDMD) algorithm extends the Exact Dynamic Mode Decomposition (DMD) method by integrating time-delay embedding and data stacking techniques. This process involves the formation of an augmented data matrix $\mathbf{X}^{\text{aug}}$, which has an increased row dimension due to the stacking of $\mathbf{X}$ from (1) and (2). The data matrix is augmented using a shift stacking and time delay matrix, drawing inspiration from the Hankel matrix in the Eigenvalue Realization Algorithm (ERA), leading to a more precise solution. The augmentation not only improves the accuracy of the solution but also expands the dimension of the measurement matrix, enabling the capture of additional data information. The augmented data matrix, which combines turn stacking and time delay, is represented as:

$$\mathbf{X}_1^{\text{aug}} = \begin{bmatrix} x_1 & x_2 & \dots & x_{n-s} \\ x_2 & x_3 & \dots & x_{n-s+1} \\ \vdots & \vdots & \ddots & \vdots \\ x_s & x_{s+1} & \dots & x_{n-1} \end{bmatrix} \tag{16}$$

$$\mathbf{X}_2^{\text{aug}} = \begin{bmatrix} x_2 & x_3 & \dots & x_{n-s+1} \\ x_3 & x_4 & \dots & x_{n-s+2} \\ \vdots & \vdots & \ddots & \vdots \\ x_{s+1} & x_{s+2} & \dots & x_n \end{bmatrix} \tag{17}$$

Here, $\mathbf{X}_1^{\text{aug}}, \mathbf{X}_2^{\text{aug}} \in \mathbb{R}^{m\cdot s\times n-s}$, where s represents the time shift, and an increment in m captures phase information for a pair of eigenvalues linked with dynamic oscillations if m is limited to $m << n$. Augmented matrices allow for the application of the DMD procedure to estimate the operator $\mathbf{F}$ in (2), resulting in the following expressions:

$$\mathbf{X}_1^{\text{aug}} = \mathbf{U}\mathbf{\Sigma}\mathbf{V}^T \tag{18}$$

$$\mathbf{F}^{\text{aug}} = \mathbf{U}^T\mathbf{X}_2^{\text{aug}}\mathbf{V}\mathbf{\Sigma}^{-1} \tag{19}$$

DMD on augmented matrices $\mathbf{X}_1^{\text{aug}}$ and $\mathbf{X}_2^{\text{aug}}$ provides the eigenvalues $\lambda_j \in \mathbf{\Lambda}_{\text{aug}}$ and modes $\mathbf{\Phi}_{\text{aug}}$. The exact dynamic modes were obtained from (12).

Using (2) with continuous eigenvalues ω_j, it is possible to reconstruct a matrix $\mathbf{X}_{\text{rec}}$ given as

$$\mathbf{X}_{\text{rec}}^{\text{aug}} = \mathbf{\Phi}_{\text{aug}} \exp(\mathbf{\Omega}_{\text{aug}} t)\mathbf{a} \tag{20}$$

where $\mathbf{a}$ are the coefficients obtained from $\mathbf{a} = \mathbf{x}_{j,1}\mathbf{\Phi}_{\text{aug}}^{-1}$. As the columns of $\mathbf{\Phi}_{\text{aug}}$ are stacked s times, their dimensions are significantly larger than the original measurements. Thus, the current-state DMD modes must be extracted from $\mathbf{\Phi}_{\text{aug}}$ by retrieving the first m rows.

2.3. Forward-Backward Dynamic Mode Decomposition

The Forward-Backward Dynamic Mode Decomposition (fbDMD) is an extension of the DMD algorithm that aims to approximate the cancellation of noise in the data and reduce error by calculating the low-rank linear operator as the square root of the product of the operators for forward and backward evolution. This method is expected to yield superior results with higher precision in computing eigenvalues and eigenvectors compared to the conventional DMD method.

The fbDMD comprises two primary steps: Forward DMD and Backward DMD. In the Forward DMD, two observation matrices, $\mathbf{X}_1$ and $\mathbf{X}_2$, are considered, which are taken at different time snapshots. The SVD factorization of $\mathbf{X}_1$ can be expressed as follows

$$\mathbf{X}_1 = \mathbf{U}\mathbf{\Sigma}\mathbf{V}^T \tag{21}$$

The projected data matrices are calculated as

$$\tilde{\mathbf{X}}_1 = \mathbf{U}\mathbf{X}_1 \tag{22}$$

$$\tilde{\mathbf{X}}_2 = \mathbf{U}\mathbf{X}_2 \tag{23}$$

The decomposition of the matrices $\tilde{\mathbf{X}}_1$ and $\tilde{\mathbf{X}}_2$ can be expressed as

$$\tilde{\mathbf{X}}_1 = \mathbf{U}_1\mathbf{\Sigma}_1\mathbf{V}_1^T \tag{24}$$

$$\tilde{\mathbf{X}}_2 = \mathbf{U}_2\mathbf{\Sigma}_2\mathbf{V}_2^T \tag{25}$$

The transformation matrix formed from the forward computation is denoted by $\mathbf{F}_f$. The dynamic mode is computed by taking the matrix formed from the succeeding time intervals, hence the term 'forward' DMD. In this step, $\tilde{\mathbf{X}}_2$ is used to estimate the transformation matrix by considering the results of the SVD of $\tilde{\mathbf{X}}_1$. The matrix $\mathbf{F}_f$ is considered to share the same eigendecomposition as $\mathbf{F}$, and can be expressed as

$$\tilde{\mathbf{F}}_f = \mathbf{U}_1^T\tilde{\mathbf{X}}_2\mathbf{V}_1\mathbf{\Sigma}_1^{-1} \tag{26}$$

The Backward DMD is analogous to the Forward DMD technique, with the major difference being the backward computation of the transformation matrix. In this case, $\tilde{\mathbf{X}}_2$ is the snapshot matrix which is factorized through SVD rather than $\tilde{\mathbf{X}}_1$. $\tilde{\mathbf{X}}_1$ is rewritten using the modified $\tilde{\mathbf{X}}_2$. From these considerations, the similar transformation matrix using the backward time shifts is obtained as

$$\tilde{\mathbf{F}}_b = \mathbf{U}_2^T\tilde{\mathbf{X}}_1\mathbf{V}_2\mathbf{\Sigma}_2^{-1} \tag{27}$$

Here, $\mathbf{F}_b$ is the transformation matrix formed from the backward computation, hence the term 'backward' DMD.

Finally, by using Forward-DMD and Backward-DMD, $\mathbf{F}$ is computed as

$$\mathbf{F} = \sqrt{\mathbf{F}_f\mathbf{F}_b^{-1}} \tag{28}$$

The matrix $\mathbf{F}$ is the computed transformation matrix used to find the dynamic mode matrix $\mathbf{\Phi}$ as follows:

$$\mathbf{\Phi}_{FB} = \mathbf{X}_2\mathbf{V}\mathbf{\Sigma}^{-1}\mathbf{W} \tag{29}$$

The eigenvalue decomposition of $\mathbf{F}$ gives the DMD damping and frequencies. From the results obtained, the damping and angular frequencies can be calculated using the logarithmic mapping of the eigenvalues described in (15). Finally, the reconstructed matrix

is obtained in (30) from the dynamic mode matrix $\mathbf{\Phi}_{FB}$ and the continuous eigenvalues $\mathbf{\Omega}_{FB}$.

$$\mathbf{X}_{\text{rec}}^{FB} = \mathbf{\Phi}_{FB} \exp(\mathbf{\Omega}_{FB} t)\mathbf{a} \tag{30}$$

2.4. Total Dynamic Mode Decomposition (tDMD)

The Total Dynamic Mode Decomposition (tDMD) method is primarily applied in noise-dominated scenarios. It addresses noise mitigation by aligning two shifted data sequences, $\mathbf{X}_1$ and $\mathbf{X}_2$, representing snapshots of a signal[3]. $\mathbf{X}_1$ is assumed to be noise-affected, while $\mathbf{X}_2$ is considered noise-free. Through a least-squares approach, DMD seeks a linear correlation between the snapshots, treating $\mathbf{X}_2$ as the reference. This asymmetric relationship forms a total least-squares problem[12]. Stacked data is initially formed as:

$$\mathbf{Z} = [\mathbf{X}_1 \ \mathbf{X}_2]^T \tag{31}$$

The problem is addressed by projecting $\mathbf{X}_1$ and $\mathbf{X}_2$ onto the optimal r-dimensional subspace using SVD, enhancing spectral information extraction:

$$\tilde{\mathbf{X}}_2 = \mathbf{X}_1\mathbf{V} \tag{32}$$

$$\tilde{\mathbf{X}}_2 = \mathbf{X}_2\mathbf{V} \tag{33}$$

If $\tilde{\mathbf{X}}_1$ undergoes SVD:

$$\tilde{\mathbf{X}}_1 = \mathbf{U}_r\mathbf{\Sigma}_r\mathbf{V}_r^T \tag{34}$$

then the DMD operator matrix $\mathbf{F}$ is determined as:

$$\mathbf{F} = \mathbf{U}_r^T\mathbf{X}_2\mathbf{V}_r\mathbf{\Sigma}_r^{-1} \tag{35}$$

$\mathbf{F}$ characterizes the system's behavior, leading to exact dynamic mode matrix $\mathbf{\Phi}_T$ computation similarly as (12). Damping and frequency are then obtained from (13). Ultimately, the reconstructed matrix $\mathbf{X}_{\text{rec}}$ with continuous eigenvalues is defined as follows:

$$\mathbf{X}_{\text{rec}}^T = \mathbf{\Phi}_T \exp(\mathbf{\Omega}_T t)\mathbf{a} \tag{36}$$

2.5. Randomized Dynamic Mode Decomposition (rDMD)

The Randomized Dynamic Mode Decomposition (rDMD) integrates a randomized methodology into the conventional DMD approach[4]. The core concept is to employ randomness as a computational tool to derive a compressed representation, referred to as a "sketch." This condensed matrix sketch serves as the basis for computing an approximate low-rank factorization of the high-dimensional data matrix. The rDMD exploits established probabilistic techniques to compute the optimal orthonormal basis $\mathbf{Q}$ using the randomization strategy[13].

Given a target rank $r \ll \min(m,n)$, the objective is to find a nearly optimal basis $\mathbf{Q} \in \mathbb{C}^{m\times r}$ for the input matrix $\mathbf{X} \in \mathbb{R}^{m\times n}$ satisfying the relation:

$$\mathbf{X} \approx \mathbf{Q}\mathbf{Q}^T\mathbf{X} \tag{37}$$

where $\mathbf{H} = \mathbf{Q}^T\mathbf{X}$, and $\mathbf{H} \in \mathbb{R}^{r\times n}$ serves as the representation of $\mathbf{X}$. To accomplish this, a test matrix $\mathbf{\Upsilon} \in \mathbb{R}^{m\times r}$ is generated from a standard Gaussian distribution to sample the range of $\mathbf{X}$, projecting the original high-dimensional data onto a random matrix:

$$\mathbf{Z} = \mathbf{X}\mathbf{\Upsilon} \tag{38}$$

Here, $\mathbf{Z}$ consists of linearly independent vectors spanning the range of $\mathbf{X}$. To ensure that the column space of $\mathbf{Q}$ spans $\mathbf{X}$ adequately, the desired range r is slightly oversampled by a constant factor p representing additional samples, typically $p = 10$[13]. Consequently, the matrix $\Psi \in \mathbb{R}^{m\times l}$ is redefined, where $l = k+p$. The QR-decomposition is then employed to obtain the desired basis $\mathbf{Q}$:

$$\mathbf{Z} = \mathbf{Q}\mathbf{R} \tag{39}$$

To enhance performance, power iterations can be applied as an alternative approach. Power iterations preprocess the input matrix to promote a faster decay of the singular value spectrum, thereby improving the quality of the approximated basis matrix $\mathbf{Q}$. The resulting sampling matrix is given by:

$$\mathbf{Z} = (\mathbf{X}\mathbf{X}^T)^q\mathbf{X}\mathbf{\Upsilon} \tag{40}$$

where q represents the number of power iterations. Even a small number of power iterations (e.g., $q = 2$) can significantly enhance the approximation quality, particularly for input matrices with slowly decaying singular values.

Once the matrix $\mathbf{Q}$ is obtained, DMD is performed in the reduced-dimensional space. The low-dimensional snapshots $\mathbf{H}$ are aggregated into overlapping matrices $\mathbf{H}_1$ and $\mathbf{H}_2$. Subsequently, applying the SVD procedure in (7) estimates the operator $\mathbf{F}$ similarly as (9), resulting in:

$$\mathbf{H}_1 = \mathbf{U}\mathbf{\Sigma}\mathbf{V}^T \tag{41}$$

$$\mathbf{F} = \mathbf{U}^T\mathbf{H}_2\mathbf{V}\mathbf{\Sigma}^{-1} \tag{42}$$

Finally, eigendecomposition is implemented to obtain the system eigenvalues and eigenvectors, enabling the extraction of continuous eigenvalues $\mathbf{\Omega}_R$, and DMD modes $\mathbf{\Phi}_R$ as described in (12), and then the damping and frequency are obtained similarly to (15). The reconstructed matrix is then obtained following (2) as

$$\mathbf{X}_{\text{rec}}^R = \mathbf{\Phi}_R \exp(\mathbf{\Omega}_R t)\mathbf{a} \tag{43}$$

3. Results

This section explains the ability of the different DMD techniques to analyze electromechanical oscillation in the modified IEEE 10-machine 39-bus system, with pumped storage hydropower plants (PSHP) based on doubly fed induction machine (DFIM) known as variable speed and Doubly-fed induction generator (DFIG) wind power simultaneously connected to bus 30 (100 MW wind power and 243 MW PSHP)[14] implemented in DIgSILENT PowerFactory. The experiments are verified using matrix $\mathbf{X}$ obtained from the voltage magnitude of each generator, affected by a fault at bus 22 ($t = 10$ to 10.15 s) with a sampling frequency $f_s = 100$ Hz. Fig. 1 illustrates the time series of the voltage magnitude of the nine generators, the voltage of the PSHP, and wind power. The results of the evaluations are compared between DMD methods to highlight the most efficient technique on three pivotal aspects: reconstruction accuracy, noise robustness, and computational cost. The different DMD algorithms were coded in MATLAB and executed on a computer with 16 GB of RAM and a 3.6 GHz Intel Core i5 processor.

3.1. Accuracy Assessment of DMD Reconstruction

The accuracy assessment of DMD algorithms involves a comparison between the original data matrix, denoted as $\mathbf{X}$, and its reconstructed counterpart, $\mathbf{X}_{\text{rec}}$. Specifically, we focus on the voltage magnitude time series stored within the data snapshot matrix, along with the associated eigenvectors. The reconstruction error is quantified as the discrepancy between $\mathbf{X}$ and $\mathbf{X}_{\text{rec}}$. Mathematically, the reconstruction percentage error is estimated using the relative norm of the Frobenius error:

$$\text{Percentage error} = \frac{|\mathbf{X} - \mathbf{X}_{\text{rec}}|_F}{|\mathbf{X}|_F} \times 100\% \tag{44}$$

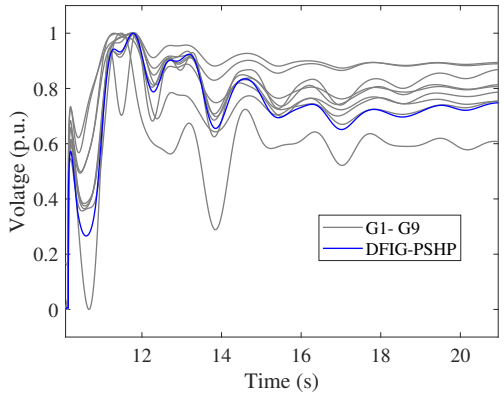

Fig. 1. Voltage magnitude of each generator from IEEE 10-machine 39-bus system.

In this study, the impact of noise levels on the matrix **X** was investigated in time windows of 6s (t=11 to 17s). Specifically, **X** was subjected to varying signal-to-noise ratio (SNR) conditions, spanning a range of 50 dB to 30 dB for all DMD methods to compare accuracy between techniques.

The difference between tDMD and rDMD methods and the other techniques is that the svdDMD, augDMD, and fbDMD methods reconstruct the snapshot **X** with all the eigenvalues whereas the tDMD and rDMD methods use only the optimum r eigenvalues for the reconstruction of the snapshot data in this work. These findings emphasize the impact of noise levels on DMD performance and provide insights for practical applications in electromechanical oscillation analysis.

Reconstruction error between the DMD methods as a function of the noise are compared with each other and listed in Fig. 2. The reconstruction error increases as the number of the noise is increased up to 30dB. The reconstruction error from the svdDMD, augDMD, and fbDMD methods is appreciably lower than that of the tDMD and rDMD methods, for all the nivels of noise. It implies that the svdDMD, augDMD, and fbDMD techniques provide higher accuracy than the DMD and rDMD approaches in predicting frequencies and modes applied to the conditions of this system.

3.2. Frequency and Damping Analysis

In this analysis, we compared the frequency and damping coefficients in a no-noise condition of the dominant resonant mode found by the DMD methods, which is listed in Table 1. The damping coefficient represents the rate of growth or decay of oscillations and is closely linked to the stability of the system. Negative damping coefficients correspond to stable oscillations, while positive coefficients indicate unstable oscillations.

The svdDMD, augDMD, and fbDMD approaches provide better results in obtaining the LFOs frequencies when compared to tDMD and rDMD methods, and are shown in Table 2 for noise condition scenarios. In pursuit of capturing the utmost spatial and temporal intricacies inherent in noisy signals, we turn our attention to matrices that approach square dimensions. Specifically, when a matrix exhibits near-square properties, SVD becomes a powerful tool for extracting dominant characteristic frequency components. Consequently, the augDMD method, which operates on larger matrices, demonstrates improved performance in estimating both frequency and damping with shift-stacking $s = 20$.

3.3. Computational time comparison

The comparative analysis of the computational efficiency of various DMD methods is presented. Specifically, it focuses on its computation time when applied to the case study under consideration. The results are summarized in Fig. 3. Among the DMD variants, augDMD exhibits a longer calculation time. This increased computational cost can be attributed primarily to the augmented matrix **X** process and the subsequent projection calculations required to obtain the operator **F**. Notably, the methods that initially project onto the $\mathbf{X}_1$ and $\mathbf{X}_2$ matrices, such as rDMD and tDMD, also incur the highest computational overhead as a consequence to find the optimum rank, r.

4. Conclusion

Ensuring grid stability is critical for efficient power transmission and secure grid operation. Achieving stability necessitates vigilant monitoring and effective mitigation of inter-area oscillation modes. Therefore, robust and efficient techniques are necessary.

In this study, we investigated the application of DMD techniques to analyze inter-area oscillations in a modified 39 IEEE bus system. Our investigation focused on on three critical aspects: reconstruction accuracy, noise robustness, and computational cost. Notably, employing the data change stacking technique led to improved accuracy by augmenting the data matrix for the aaugDMD method. However, it is crucial to recognize that the selection of the stack number can impact the emergence of spurious frequencies.

Despite the inherent robustness of methods such as fbDMD, tDMD, and rDMD against noise, their performance remains constrained by the size of the data stack required for accurate modal parameter estimation. Conversely, fbDMD, tDMD, and rDMD exhibit shorter

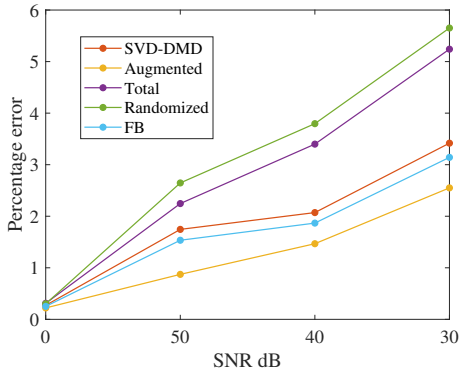

Fig. 2. Reconstruction comparison of DMD approaches for 30 of noise.

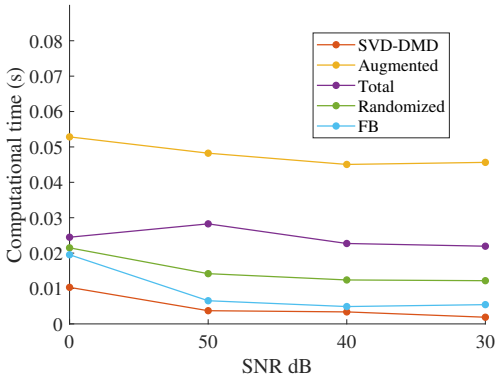

Fig. 3. DMD algorithm computational time comparison

Table 1. Dominant frequency f (Hz) and damping ρ.

svdDMD		augDMD		tbDMD		rDMD		fbDMD	
f	ρ	f	ρ	f	ρ	f	ρ	f	ρ
0.657	−0.340	0.6467	−0.482	0.657	−0.340	0.657	−0.348	0.660	−0.342

Table 2. Frequency f (Hz) and damping ρ in noise conditions.

Noise	svdDMD		augDMD		tDMD		rDMD		fbDMD	
dB	f	ρ	f	ρ	f	ρ	f	ρ	f	ρ
50	0.692	−0.357	0.669	−0.363	0.690	−0.477	0.692	−0.467	0.678	−0.388
40	0.605	−0.466	0.638	−0.378	0.659	−0.479	0.605	−0.477	0.650	−0.404
30	0.594	−0.432	0.619	−0.382	0.507	−0.510	0.483	−0.432	0.637	−0.592

computational times compared to augDMD. Our findings underscore the necessity of incorporating the data stacking matrix into each technique to further enhance performance, leveraging the mathematical framework that permits such modifications. However, judicious stack number selection remains pivotal for achieving optimal results.

References

[1] P. Esquivel, E. Barocio, M. A. Andrade, and F. Lezama, *Complex Empirical Orthogonal Function Analysis of Power System Oscillatory Dynamics*, A. R. Messina, ed. pp. 159–187. Springer US, 2009.

[2] J. H. Tu, C. W. Rowley, D. M. Luchtenburg, S. L. Brunton, and J. N. Kutz, "On dynamic mode decomposition: Theory and applications," *Journal of Computational Dynamics*, vol. 1, no. 2, pp. 391–421, 2014.

[3] S. T. M. Dawson, M. S. Hemati, M. O. Williams, and C. W. Rowley, "Characterizing and correcting for the effect of sensor noise in the dynamic mode decomposition," *Experiments in Fluids*, vol. 57, no. 42, 2016.

[4] N. B. Erichson, L. Mathelin, J. N. Kutz, and S. L. Brunton, "Randomized dynamic mode decomposition," *SIAM Journal on Applied Dynamical Systems*, vol. 18, no. 4, pp. 1867–1891, 2019.

[5] E. Barocio, B. C. Pal, N. F. Thornhill, and A. R. Messina, "A dynamic mode decomposition framework for global power system oscillation analysis," *IEEE Transactions on Power Systems*, vol. 30, no. 6, pp. 2902–2912, 2015.

[6] V. Priyanga, M. Chandni, N. Mohan, and K. Soman, "Data-driven analysis for low frequency oscillation identification in smart grid using fb-dmd and t-dmd methods," in *2019 9th International Conference on Advances in Computing and Communication (ICACC)*, pp. 51–57, 2019.

[7] A. Alassaf and L. Fan, "Randomized dynamic mode decomposition for oscillation modal analysis," *IEEE Transactions on Power Systems*, vol. 36, no. 2, pp. 1399–1408, 2021.

[8] C. W. Rowley, I. Mezić, S. Bagheri, P. Schaltter, and D. S. Henningson, "Spectral analysis of nonlinear flows," *Journal of Fluid Mechanics*, vol. 641, p. 115–127, 2009.

[9] P. J. Schmid, "Dynamic mode decomposition of numerical and experimental data," *Journal of Fluid Mechanics*, p. 5–28, 2010.

[10] E. Barocio, J. Romero, R. Betancourt, P. Korba, and F. R. S. Sevilla, *Wide-Area Monitoring of Large Power Systems Based on Simultaneous Processing of Spatio-Temporal Data*, pp. 189–228. Springer International Publishing, 2021.

[11] J. N. Kutz, S. L. Brunton, B. W. Brunton, and J. L. Proctor, *Dynamic Mode Decomposition: Data-Driven Modeling of Complex Systems*. SIAM, 2016.

[12] M. S. Hemati, C. W. Rowley, E. A. Deem, and L. N. Cattafesta, "De-biasing the dynamic mode decomposition for applied koopman spectral analysis of noisy datasets," *Theor. Comput. Fluid Dyn.*, vol. 31, pp. 349–368, 2017.

[13] N. Halko, P. G. Martinsson, and J. A. Tropp, "Finding structure with randomness: Probabilistic algorithms for constructing approximate matrix decompositions," *SIAM Review*, vol. 53, no. 2, pp. 217–288, 2011.

[14] M. Alizadeh Bidgoli, S. Atrian, W. Yang, and F. M. Gonzalez-Longatt, *Transient Stability Assessment of Power System Incorporating DFIM-Based Pumped Storage Hydropower and Wind Farm*, pp. 131–152. Springer International Publishing, 2021.